Sources of Uncertainty in Isotope Ratio Measurements by Inductively Coupled Plasma Mass Spectrometry

ARTICLE *in* ANALYTICAL CHEMISTRY · AUGUST 2001

Impact Factor: 5.64 · DOI: 10.1021/ac001537y · Source: PubMed

3 AUTHORS, INCLUDING:

Petra Lagerkvist
Swedish Defence Research Agency
13 PUBLICATIONS **227** CITATIONS
SEE PROFILE

Ilia Rodushkin
ALS Scandinavia AB and Lulea University of T…
117 PUBLICATIONS **2,809** CITATIONS
SEE PROFILE

Anal. Chem. **2001,** *73,* 2911−2919

Sources of Uncertainty in Isotope Ratio Measurements by Inductively Coupled Plasma Mass Spectrometry

Petra K. Appelblad,[†] Ilia Rodushkin,[‡] and Douglas C. Baxter*,[†]

Division of Inorganic Chemistry and SGAB Analytica, Luleå University of Technology, S-971 87 Luleå, Sweden

A model is presented describing the effects of dead time and mass bias correction factor uncertainties, flicker noise, and counting statistics on isotope ratio measurement precision using inductively coupled plasma mass spectrometry (ICPMS) with a single collector. Noise spectral analysis is exploited to enable estimation of the flicker noise parameters. For the instrument used, the flicker noise component exhibited a fairly weak frequency (f) dependence ($\propto f^{-0.33\pm0.12}$), but was directly proportional to the total number of counts, Q. As white noise, determined by counting statistics, is given by $Q^{0.5}$, the isotope ratio measurement uncertainties will actually cease to improve when Q exceeds a certain threshold. This would suggest that flicker noise could become the limiting factor for the precision with which isotope ratios can be determined by ICPMS. However, under most experimental conditions, uncertainties associated with mass discrimination and dead time correction factors are decisive. For ratios up to ~22 (^{115}In/^{113}In), optimum major isotope count rates are generally below 0.3 MHz, for which precision in the mass discrimination factor is limiting. The model derived could be used as a starting point for determining optimum conditions and understanding the limitations of single-collector ICPMS for precise isotope ratio measurements.

Since the introduction of inductively coupled plasma mass spectrometry (ICPMS), one of the important application goals has been the measurement of isotope ratios with high precision.[1−4] This goal has remained rather elusive, as the typical instrumental configuration, with a single collector, can rarely perform on a par with the benchmark technique for precise elemental isotope ratio determination, thermal ionization mass spectrometry (TIMS).[3,4] The major problem with ICPMS stems from the instability of the ion source and the sequential, albeit rapid, sampling of the ion beams.[2−6] On the other hand, the efficiency of the plasma as an ion source means that a greater number of elements are accessible to isotopic analysis by ICPMS.[7] This advantage is one of the driving forces behind the continued interest in isotope ratio measurement by ICPMS and has culminated in the development of multicollector (MC) instruments that yield precision values comparable with TIMS.[6,7] Nevertheless, the precision attainable using single-collector ICPMS is sufficient for many applications.[8,9]

Currently, the expense of MC-ICPMS systems prohibits their more widespread use in analytical laboratories. Consequently, there is still a need to be able to carry out isotopic analyses using conventional, single-collector ICPMS with the smallest possible uncertainties. In the ideal case, measurement precision would be limited purely by counting statistics, although in practice, source fluctuations provide a considerable flicker noise contribution to the overall uncertainty.[2,3,5] Isotope ratios measured by ICPMS must also be corrected for detector dead time, when data are acquired in the counting mode[3,10] to enable measurement at low abundances, and for mass discrimination, due to the differential transmission efficiencies as a function of mass and ion beam composition.[4,11−13] These correction factors must be determined experimentally and will thus be associated with uncertainties.[11,14]

In this study, a model including the flicker noise contribution to isotope ratio uncertainties by ICPMS is derived and experimentally evaluated. The model is then extended to account for dead time and mass discrimination correction factor uncertainties. It is shown that the latter often dominate over the actual isotope ratio measurement uncertainties, suggesting that the precision values quoted for ICPMS are frequently overly optimistic.

THEORETICAL SECTION

Measurement Noise Contributions to Isotope Ratio Uncertainties. To be able to predict the effects of data acquisition

* Corresponding author: (e-mail) Douglas.Baxter@km.luth.se.
[†] Division of Inorganic Chemistry.
[‡] SGAB Analytica.

(1) Russ, G. P., III; Bazan, J. M.; Date, A. R. *Anal. Chem.* **1987**, *59*, 984−989.
(2) Crain, J. S.; Houk, R. S.; Eckels, D. E. *Anal. Chem.* **1989**, *61*, 606−612.
(3) Begley, I. S.; Sharp, B. *J. Anal. At. Spectrom.* **1994**, *9*, 171−176.
(4) Heumann, K. G.; Gallus, S. M.; Rädlinger, G.; Vogl, J. *J. Anal. At. Spectrom.* **1998**, *13*, 1001−1008.
(5) Ince, A. T.; Williams, J. G.; Gray, A. L. *J. Anal. At. Spectrom.* **1993**, *8*, 899−903.
(6) Waldner, A. J.; Freedman, P. A. *J. Anal. At. Spectrom.* **1992**, *7*, 571−575.
(7) Halliday, A. N.; Lee, D. C.; Christensen, J. N.; Rehkämper, M., Yi. W.; Luo, X.; Hall, C. M., Ballentine, C. J.; Pettke, T.; Stirling, C. *Geochim. Cosmochim. Acta* **1998**, *62*, 919−940.
(8) Barnes, R. *Fresenius J. Anal. Chem.* **1996**, *355*, 433−441.
(9) Becker, J. S.; Dietze, H. J. *J. Anal. At. Spectrom.* **1998**, *13*, 1057−1063.
(10) Hayes, J. M.; Schoeller, D. A. *Anal. Chem.* **1977**, *49*, 306−311.
(11) Begley, I. S.; Sharp, B. *J. Anal. At. Spectrom.* **1997**, *12*, 395−402.
(12) Gillson, G. R.; Douglas, D. J.; Fulford, J. E.; Halligan, K. W.; Tanner, S. D. *Anal. Chem.* **1988**, *60*, 1472−1474.
(13) Tanner, S. D. *Spectrochim. Acta* **1992**, *47B*, 809−823.
(14) Appelblad, P. K.; Baxter, D. C. *J. Anal. At. Spectrom.* **2000**, *15*, 557−560.

10.1021/ac001537y CCC: $20.00
Published on Web 05/24/2001

parameters on isotope ratio measurement precision, a model describing the relevant uncertainty contributions is required. From the literature,[2,3,5] the two dominant sources of uncertainty are unanimously identified as white noise, associated with the ion counting process, and flicker ($1/f$) noise, originating in the ICP. Additional noise contributions are made, at discrete spectral frequencies, by the sample introduction or nebulizer drainage system, mains pickup, and the plasma audio frequency. For the present purposes, only white and flicker noise will be considered further.

An initial assumption is made that the total noise, σ_{Tot}, on the detected signal is related to the sum of squares of the white (σ_{wh}) and flicker (σ_{f}) noise components:[15−18]

$$\sigma_{\mathrm{Tot}} = (\sigma_{\mathrm{wh}}{}^2 + \sigma_{\mathrm{f}}^2)^{0.5} \quad (1)$$

From Poisson statistics,[3,15−18] the white noise contribution, which is independent of frequency, can be expressed as

$$\sigma_{\mathrm{wh}} = (It_d n_{\mathrm{p}} n_{\mathrm{s}})^{0.5} = (Itn_{\mathrm{s}})^{0.5} = Q^{0.5} \quad (2)$$

where I (Hz) is the measured count rate, the signal being accumulated during the dwell time (t_{d}, s) and over a defined number of scans (n_{s}) and points per peak (n_{p}) yielding a total number of counts, Q, as the product of these parameters. Note that eq 2 is valid for the flat-topped peaks generated by sector field ICPMS (in low-resolution mode) and not strictly so for the peak shapes obtained using quadrupole-based instruments.[11,19] The root-mean-square flicker noise is described by the following relationship[16]

$$\sigma_{\mathrm{f}} = (\xi Q^a \int_{f_{\mathrm{L}}}^{f_{\mathrm{U}}} f^{-n}\, \mathrm{d}f)^{0.5} = (A \int_{f_{\mathrm{L}}}^{f_{\mathrm{U}}} f^{-n}\, \mathrm{d}f)^{0.5} \quad (3)$$

where ξ is a constant, termed the flicker factor,[15] that depends on the system under study, the exponent a is close to 2, n is typically less than 1, and f is the frequency (Hz). In most texts on noise analysis, the exponent a is assumed to equal 2.[15,17] The limits of the integral term are defined below.

In isotope ratio measurements using a single-collector ICPMS instrument, noise reduction effects are operational.[3] For a pair of isotopes, denoted by subscripts M (major) and m (minor), the elapse time, t_{e} (s), from the onset of measurement of the first isotope to the end of measurement of the second is given by the following: $t_{\mathrm{e}} = (t_{\mathrm{dM}} + t_{\mathrm{dm}})n_{\mathrm{p}} + t_{\mathrm{s}}$. Here t_{s} (s) is the mass spectrometer settling time for shifting between masses. It is assumed that the time spent acquiring data at each of the two masses may differ to improve the counting statistics for the least abundant isotope.[20]

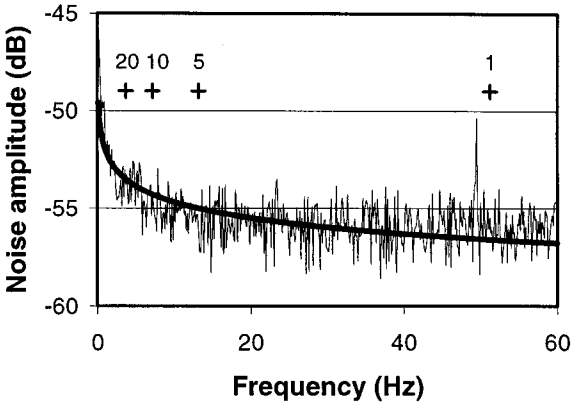

Figure 1. Noise amplitude spectrum for $^{115}In^+$ acquired at an average count rate of 715 ± 6 kHz. The thick solid line shows the noise calculated using the model described by eqs 1−3 and the parameters from Table 2. Crosses mark the central frequencies around which the noise would be sampled from the minor isotope noise spectrum for the indicated dwell time ratios, with $t_{\mathrm{M}} = 0.002$ s.

Isotope ratioing will reduce noise by providing a low-frequency cutoff [3,15]

$$f_1 = 1/2\pi t_{\mathrm{e}} \quad (4)$$

This will eliminate a portion of the low-frequency flicker noise. An upper frequency cutoff for each individual isotope is determined by the time spent acquiring data:

$$f_2 = 1/2\pi t \quad (5)$$

Under conditions typical of isotope ratio measurement by ICPMS, this upper cutoff will remove high-frequency noise peaks, above ∼100 Hz, such as plasma audio frequency and higher harmonics of mains pickup.[2,3,5] The noise rejection capabilities provided by isotope ratioing have the characteristics of a band-pass filter[3] with a noise equivalent bandwidth, Δf (Hz), given by[15]

$$\Delta f = (\pi/2n_{\mathrm{s}})(f_2 - f_1) \quad (6)$$

and centered at the average of the upper and lower cutoff frequencies. Note that, when the dwell times for the isotopes are not identical, different regions of the noise spectrum will be sampled in the two measurements to be ratioed (see Figure 1). This means that f_2 and Δf, given by eqs 4 and 6, will have different values depending on the two dwell times, t_{dM} and t_{dm}. Increasing the number of scans included in the ratio measurement will improve the noise rejection capabilities by multiple time averaging, which effectively reduces the noise equivalent band-pass.[3,18] Ingle and Crouch[15] have given a thorough and accessible account of noise sources and frequency characteristics of signal processing systems.

The lower and upper cutoff frequencies, as well as Δf, define the actual flicker noise contribution to the total noise in the

(15) Ingle, J. D., Jr.; Crouch, S. R. *Spectrochemical Analysis*; Prentice Hall: Englewood Cliffs, NJ, 1988; Chapter 5, pp 135−163.
(16) Pettai, R. *Noise in Receiving Systems*; Wiley: New York, 1984; Chapter 2, pp 4−16.
(17) Seller, P. *Nucl. Instrum. Methods Phys. Res.* **1996**, *376A*, 229−241.
(18) Wilmshurst, T. H. *Signal Recovery from Noise in Electronic Instrumentation*; Hilger: Bristol, U.K., 1985; Chapter 6, pp 69−90.
(19) Turner, P. J.; Mills, D. J.; Schröder, E.; Lapitajs, G.; Jung, G.; Iacone, L. A.; Haydar, D. A.; Montaser, A. In *Inductively Coupled Plasma Mass Spectrometry*; Montaser, A., Ed.; Wiley: New York, 1988; Chapter 6, pp 421−501.
(20) Koirtyohann, S. R. *Spectrochim. Acta* **1994**, *49B*, 1305−1311.

measured signal under the specified instrumental conditions. Equation 3 must be integrated over the noise equivalent bandwidth using the appropriate frequency limits[15,18]

$$f_L = {}^1/_2(f_1 + f_2 - \Delta f) = f_c - {}^1/_2\Delta f \quad (7)$$

$$f_U = {}^1/_2(f_1 + f_2 + \Delta f) = f_c + {}^1/_2\Delta f \quad (8)$$

The central frequency for noise acceptance, f_c (Hz), is given by the average of f_1 and f_2.[15]

The theoretical value of the standard error (SE $= \sigma/N^{0.5}$) in the measured isotope ratio, $R_{meas} = Q_M t_m / Q_m t_M$, is usually expressed on the basis of assumed Poisson distributions of the total counts acquired for each isotope as the only noise sources:

$$\mathrm{SE}(R_{meas})_{Poisson} = \frac{t_m}{t_M}\left[\frac{{\sigma_{wh,M}}^2}{N}\left(\frac{1}{Q_m}\right)^2 + \frac{{\sigma_{wh,m}}^2}{N}\left(\frac{Q_M}{{Q_m}^2}\right)^2\right]^{0.5} \quad (9)$$

i.e., only white noise contributions are considered (N is the number of measurements of the ratio collected). The calculated standard error in the measured ratio, including the flicker noise contribution, can be computed from the expression

$$\mathrm{SE}(R_{calc}) = \frac{t_m}{t_M}\left[\frac{{\sigma_{Tot,M}}^2}{N}\left(\frac{1}{Q_m}\right)^2 + \frac{{\sigma_{Tot,m}}^2}{N}\left(\frac{Q_M}{{Q_m}^2}\right)^2\right]^{0.5} \quad (10)$$

Neglecting the uncertainties associated with flicker noise, i.e., using eq 9 rather than eq 10 to predict the expected level of precision, serves as an explanation for the fact that, in most experimental studies, the uncertainties obtained are greater than the limits imposed by counting statistics.[3,5,20]

Note that, in the following, the standard error in the experimentally determined isotope ratio will be denoted SE(R_{expt}).

Correction Factor Contributions to Isotope Ratio Uncertainties. To obtain accurate isotope ratios in ICPMS, the counts acquired must be corrected for the detector dead time (τ, s)[10,11,20]

$$\frac{1}{Q^0} = \frac{1}{Q} - \frac{\tau}{tn_s} \quad (11)$$

The corrected isotope ratio is then given by the quotient between the dead time corrected ion signals for the major and minor isotopes, corrected for mass discrimination (κ):[4,11]

$$R_{corr} = \kappa\frac{t_m}{t_M}\frac{{Q_M}^0}{{Q_m}^0} = \kappa\frac{t_m\left(\frac{1}{Q_m} - \frac{\tau}{t_m n_s}\right)}{t_M\left(\frac{1}{Q_M} - \frac{\tau}{t_M n_s}\right)} \quad (12)$$

From eq 12 the following relationship describing the contributions of all parameters to SE(R_{corr}) can be derived:

$$\mathrm{SE}(R_{corr}) = \left\{\frac{{\sigma_{Tot,m}}^2}{N}\left[\kappa\frac{t_m}{t_M}\frac{\left(\frac{1}{Q_m}\right)^2}{\left(\frac{1}{Q_M} - \frac{\tau}{t_M n_s}\right)}\right]^2 + \frac{{\sigma_{Tot,m}}^2}{N} \times \left[\kappa\frac{t_m}{t_M}\frac{\left(\frac{1}{Q_m} - \frac{\tau}{t_m n_s}\right)}{(I_M\tau - 1)^2}\right]^2 + \mathrm{SE}(\kappa)^2\left[\frac{t_m}{t_M}\frac{\left(\frac{1}{Q_m} - \frac{\tau}{t_m n_s}\right)}{\left(\frac{1}{Q_M} - \frac{\tau}{t_M n_s}\right)}\right]^2 + \mathrm{SE}(\tau)^2\left[\kappa\frac{t_m}{t_M}\frac{\left(\frac{1}{Q_m t_M n_s} - \frac{1}{Q_M t_m n_s}\right)}{\left(\frac{1}{Q_M} - \frac{\tau}{t_M n_s}\right)^2}\right]^2\right\}^{0.5} \quad (13)$$

where SE(κ) and SE(τ) are the standard errors in the mass discrimination and dead time correction factors, respectively. Denoting the terms contributing to the total uncertainty in R_{corr} on the right-hand side of eq 13 as $u^2(Q_m)$, $u^2(Q_M)$, $u^2(\kappa)$ and $u^2(\tau)$, the relative standard error (RSE, %) is

$$\mathrm{RSE}\ (R_{corr}) = \frac{(u^2(Q_m) + u^2(Q_M) + u^2(\kappa) + u^2(\tau))^{0.5}}{R_{corr}} \times 100\% \quad (14)$$

Equations 13 and 14 are useful for calculating the uncertainties on a purely theoretical basis. However, for including the contributions of dead time and mass discrimination correction factors to the total experimental uncertainty, they are not directly applicable. This is a consequence of the fact that, for experimental measurements, better precision is achieved by calculating the ratio on a scan-by-scan or measurement-by-measurement basis, rather than using average count rates at the end of the data acquisition. Thus, it is necessary to use SE(R_{expt}) rather than the standard errors for the numbers of counts acquired for each isotope. To resolve this difficulty, eq 14 can be reformulated as follows:

$$\mathrm{RSE}\ (R_{expt,corr}) = \frac{\left\{\left(\frac{\mathrm{SE}(R_{expt})}{\mathrm{SE}(R_{calc})}\right)^2[u(Q_m)^2 + u(Q_M)^2] + u(\kappa)^2 + u(\tau)^2\right\}^{0.5}}{R_{corr}} \times 100\% \quad (15)$$

where SE(R_{calc}) is as defined by eq 10. This facilitates the correct apportionment of experimental error, but requires that all other terms in eq 15 are evaluated, which represents a considerable task.

EXPERIMENTAL SECTION

Instrumentation. All experiments were performed using a double-focusing, sector field ICPMS instrument (Element, Finnigan MAT, Bremen, Germany) operated in the low-resolution mode. The instrument is equipped with a secondary electron multiplier for ion detection, a peristaltic pump (CETAC Technologies, Omaha, NE) for drainage of the sample introduction system, a MicroMist nebulizer (Glass Expansion, Romainmotier, Switzerland), a Scott-type double-pass spray chamber, and a Fassel torch.

Table 1. Instrumental Operating Conditions

forward power	1500 W	sampling cone	nickel, 1.1-mm orifice diameter
coolant gas	13 L of Ar min^{-1}	skimmer cone	nickel, 0.8-mm orifice diameter
auxiliary gas	0.8 L of Ar min^{-1}	acquisition mode	E-scan
nebulizer gas	optimized daily		

	element				
	boron	magnesium	indium[a]	thallium	uranium
t_{dM}	5 ms for ^{11}B	10 ms for ^{24}Mg	10 ms for ^{115}In (1 ms)	10 ms for ^{205}Tl	2 ms for ^{235}U, ^{238}U
t_{dm}	10 ms for ^{10}B	10 ms for ^{25}Mg, ^{26}Mg	10 ms for ^{113}In (−)	10 ms for ^{203}Tl	20 ms for ^{234}U[b]
t_s	1 ms	1 ms	1 ms (1 ms)	1 ms	1 ms
n_p	3	3	5 (1)	5	3
n_s	1000	100	100 (1024)	100	1000
N	10	15	15 (18)	15	7

[a] Conditions applied for noise spectral analysis given in parentheses. Other deviations from these settings are noted in the relevant text. [b] Additional data were collected at mass-to-charge ratios of 233, 236, 237, 239, and 240.

Samples were introduced by self-aspiration induced by a nebulizer gas flow rate of 1.2−1.3 L min^{-1} to minimize peristaltic pump noise. Ion lens settings, sampling depth, and nebulizer gas flow rates were adjusted daily to achieve maximum signal intensity for $^{115}In^+$. Operating conditions are listed in Table 1. For all experiments, the dead time was set to zero in the instrument software. Detection was made in the counting mode throughout, count rates up to 5 MHz being permitted before the instrument automatically switches to analog mode.

Reagents and Materials. Single-element standard solutions (1000 mg L^{-1}, SPEX Plasma Standards, Edison, NJ) were used throughout. These were diluted to appropriate concentrations using deionized water (Millipore Milli-Q, Bedford, MA) and acidified to 0.14 mol L^{-1} nitric acid (p.a. grade, Merck, Darmstadt, Germany, further purified by sub-boiling distillation in a quartz still).

For determination of the mass discrimination correction factor for boron isotope ratio measurements, the isotopic reference material NBS-SRM 951 boric acid distributed by NIST (Gaithersburg, MD) was employed. Eight samples distributed by the Istituto di Geocronologia e Geochimica Isotopica (Pisa, Italy) were analyzed with respect to $^{11}B/^{10}B$ isotope ratios using ICPMS. Two samples of groundwater and one of seawater were simply diluted prior to measurement.[21] The five rock and mineral samples were prepared for analysis using methods described elsewhere.[22,23]

Four samples, containing ∼100 ng of uranium as dry uranyl nitrate, were supplied by the Institute for Reference Materials and Measurements (Geel, Belgium) in the context of the nuclear signatures interlaboratory measurement evaluation program (NUSIMEP-2: uranium isotopic ratios[24]). The solids were brought into solution using distilled nitric acid and diluted with distilled, deionized water to total uranium concentrations of ∼10 μg L^{-1}. Note that only data for ^{234}U, ^{235}U, and ^{238}U are included here, although several additional mass-to-charge ratios were also monitored, as indicated in Table 1. Mass discrimination was corrected using data acquired for NBS uranium isotopic standards U-030 and U-050.

Noise Spectral Analysis. Data acquisition was undertaken using the operating conditions given in Table 1. Measurements were made at four concentration levels yielding average count rates for $^{115}In^+$ between 0.72 and 4.19 MHz. Noise spectra were calculated by 1024-point fast Fourier transformation (FFT), taking the sum of squares of the real and imaginary components of the transformed data.[3] For presentation of data, the noise amplitude (dB), as defined by the relation[3,15]

$$\text{noise amplitude} = \log(\sigma^2_{Tot}/Q^2) \qquad (16)$$

has been utilized, to conform with previous studies.[2,3,5] The quantities σ^2_{Tot} and Q^2 were provided by the FFT. Signal averaging over 18 data sets was performed in the frequency domain. The effective data acquisition rate was 137 Hz, limited by the time taken to store the data in the instruments' computer system. The Nyquist frequency was 68.5 Hz and the resolution was 0.133 Hz.

The sum of squares was assumed to correspond to σ^2_{Tot} as defined by eq 1. For the noise spectral analysis measurements, $n_p = 1$, $n_s = 1024$, and $t_d = 1$ ms, so the white noise contribution at any given point is the product of these variables and the count rate. Thus the flicker noise contribution could be separated from the total noise as $\sigma^2_f = \sigma^2_{Tot} - \sigma^2_{wh}$. To estimate the parameters defining the flicker noise in eq 3, linear regression was employed,[25] as described in Table 2. First, A and n were evaluated by regressing log σ^2_f on log f. Then the flicker noise parameter A was broken down into ξ and a using the linear relationship between log A and log Q.

RESULTS AND DISCUSSION

Measurement Noise. An example of a noise amplitude spectrum for the ICPMS system used is shown in Figure 1. It can be seen that the appearance of this spectrum is dominated by the flicker noise component. The only other clearly discernible feature is the fundamental noise peak at 50 Hz arising from ac power line pickup.[2,3,5] It should be noted that sample introduction was achieved by self-aspiration, and so discrete noise components caused by rotation of the peristaltic pump rollers were effectively eliminated. Prior to fitting the flicker noise model of eq 3 to the

(21) Rodushkin, I.; Ruth, T. *J. Anal. At. Spectrom.* **1997**, *12*, 1181−1185.
(22) Nakamura, E.; Ishikawa, T.; Birck, J. L.; Allègre, C. *Chem. Geol.* **1992**, *94*, 193−204.
(23) Tonarini, S.; Pennisi, M.; Leeman, W. P. *Chem. Geol.* **1997**, *142*, 129−137.
(24) Held, A.; Alonso, A.; De Bolle, W.; Verbruggen, A.; Wellum, R. *NUSIMEP-2 Uranium Isotopic Abundances, Report to Participants;* EUR 19744/EN; European Commission: Geel, Belgium, 2001; pp 1−37.
(25) Miller, J. C.; Miller, J. N. *Statistics for Analytical Chemistry*, 2nd ed.; Ellis Horwood: Chichester, U.K., 1988; Chapters 3 and 5, pp 53−80, 101−137.

Table 2. Estimation of Flicker Noise Parameters in Eq 3 by Regression Analysis of ICPMS Data for ^{115}In[a]

	Estimation of A and n	
	$\log(\sigma_f^2) = \log A + n \log f$	
$\log Q$	$\log A$	n
5.8646	6.616 ± 0.036	-0.271 ± 0.027
6.2037	7.218 ± 0.038	-0.320 ± 0.029
6.5765	7.932 ± 0.037	-0.372 ± 0.028
6.6324	8.120 ± 0.024	-0.341 ± 0.030
average		-0.33 ± 0.12
	Estimation of ξ and a	
	$\log A = \log \xi + a \log Q$	
$\xi = (2.0 \pm 9.8) \times 10^{-5}$		$a = 1.93 \pm 0.33$

[a] Error terms are 95% confidence limits.

experimental data, the spectral region corresponding to the peak at 50 Hz was deleted from each data set.

The flicker noise parameters derived from noise spectral analysis at four concentration levels are reported in Table 2. These permitted calculation of σ_f^2 as a function of frequency using eq 3. In combination with the white noise contribution, yielding σ_{Tot}^2, the predicted noise amplitude could then be computed in accordance with eq 16. The modeled noise spectrum has been included in Figure 1. All modeled spectra provided highly significant fits ($P < 0.01$)[25] to the experimental data.

From Table 2 it is evident that the flicker noise is not directly inversely proportional to frequency, i.e., $n = -0.33$ rather than -1. Thus, the frequency dependence of the flicker noise component is actually fairly weak. This means that higher measurement frequencies, than are accessible with the ICPMS instrument employed here, would be required to approach the counting statistics limit for isotope ratio measurements. The results provided in Table 2 indicate that the exponent a in eq 3 is within experimental error of the expected value of 2.[16] In other words, σ_f for measurement of a given isotope is directly proportional to the total number of counts acquired, Q, whereas σ_{wh} is equivalent to $\sqrt{Q}$. The absolute magnitude of the flicker noise component is determined by ξ (2×10^{-5}; Table 2) and the integral term in eq 3, both of which are below unity. Nevertheless, as Q increases by accumulating more scans or extending dwell times, the flicker noise component will ultimately exceed the uncertainty contributions made by counting statistics. Beyond this point, isotope ratio measurement precision will actually stop improving with increasing numbers of counts.

The uncertainty in the value of the flicker noise factor, ξ, is disconcertingly large. This is a result of the logarithmically transformed data points used for linear regression analysis being clustered in a region far removed from the origin.[25] Better precision could be achieved by collecting data over a broader range, extending to lower count rates. For further calculations of flicker noise, the estimated value of ξ from Table 2 was used together with the expected value of the signal exponent; i.e., $a = 2$. As will be shown by the following results, the adopted parameter values provided acceptable agreement with the experimental observations.

Effect of Minor Isotope Dwell Time. As described in the Theoretical Section, the use of different dwell times for the major and minor isotopes, to improve the counting statistics for the latter,[20] will result in sampling of data from different regions of the noise spectrum.[18] This is illustrated in Figure 1, where it can be seen that, the longer the dwell time for the minor isotope, the more the center of the noise equivalent bandwidth shifts toward the flicker noise dominated region. It is also worth noting that f_c (51.16 Hz) for the major isotope, and potentially for the minor isotope as well if $t_m = t_M = 0.002$ s, is very close to the ac power line disturbance. Thus, depending on Δf for the experimental parameters applied, the precision of measurements could be negatively impacted by acceptance of this discrete noise peak.[3] It was observed that the magnitude of the 50-Hz noise peak increased, albeit in nonlinear fashion, with increasing analyte concentration, in agreement with the results of Ince et al.[5]

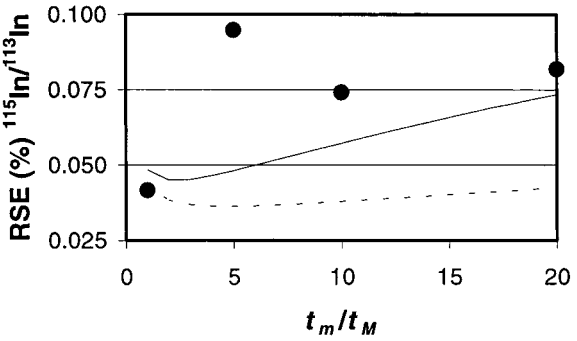

Figure 2. RSE (%) for indium isotope ratio as a function of the dwell time ratio. Variation in the RSE as predicted using the Poisson model of eq 9 is shown by the dotted line. The solid line shows the results obtained by including the flicker noise contributions in eq 10. Circles represent the experimental data acquired at dwell time ratios of 1, 5, 10 and 20; $t_M = 2$ ms; $t_s = 1$ ms; $n_p = 1$; $N = 7$; $I_M = 3.06 \pm 0.15$ MHz; $I_m = 141 \pm 7$ kHz. The number of scans was adjusted to maintain a total data acquisition time of 10 s. Data have not been corrected for dead time and mass discrimination.

For the specific case of $t_m = t_M = 2$ ms, and the measurement conditions employed to calculate the sampling frequencies shown in Figure 1, $\Delta f/2$ would be less than ($f_c - 50$) Hz for $n_s \geq 39$ scans. This example illustrates the fact that discrete noise peaks are extremely unlikely to affect the quality of ratio measurements by ICPMS, as that would require almost perfect coincidence of a noise frequency with f_c for one or both of the isotopes. Generally, considerably more scans are acquired, and the noise frequency bandwidth is therefore too narrow to accept discrete noise components. If in doubt, then it is a relatively simple matter to determine the acceptance frequency limits for the conditions of interest using eqs 4−8. In agreement with conclusions reached in previous studies of ICPMS,[2,3,5] this analysis suggests that flicker and white noise sources are dominant.

Figure 2 compares experimental and calculated RSE (%) values for raw indium isotope ratios, i.e., without correction for dead time and mass discrimination, as a function of dwell time ratio. Koirtyohann[20] has proposed that the optimum ratio of dwell times follows the relationship

$$t_m/t_M = (W_M/W_m)^{0.5} = R^{0.5} \qquad (17)$$

where W is the relative isotopic abundance. This assumes that all uncertainties can be described by counting statistics, yielding

Table 3. Isotope Ratios and Experimentally Determined Dead Time and Mass Discrimination Correction Factors

isotope pair	isotope ratio[a]	κ[b]	τ[b] (ns)
$^{11}B/^{10}B$[c]	3.9272 ± 0.0018	0.8696 ± 0.0009	24.0 ± 1.2
	4.0584 ± 0.0024	0.9328 ± 0.0004	
$^{24}Mg/^{25}Mg$[d]	7.899 ± 0.009	1.0333 ± 0.0014	21.3 ± 1.3
$^{24}Mg/^{26}Mg$[d]	7.174 ± 0.020	1.0658 ± 0.0038	22.1 ± 3.9
$^{115}In/^{113}In$	22.31 ± 0.26	0.9839 ± 0.0012	19.6 ± 1.3
$^{205}Tl/^{203}Tl$	2.3871 ± 0.0012	0.9991 ± 0.0007	17.5 ± 0.6
$^{234}U/^{238}U$[e]	$4.308 \times 10^{-5} \pm 1.5 \times 10^{-7}$	1.0056 ± 0.0003	21.0 ± 1.0
	$3.091 \times 10^{-4} \pm 1.3 \times 10^{-6}$		
$^{235}U/^{238}U$[e]	$6.2465 \times 10^{-3} \pm 3.0 \times 10^{-6}$	1.0042 ± 0.0002	21.0 ± 1.0
	$2.4592 \times 10^{-2} \pm 1.7 \times 10^{-5}$		

[a] Error terms are 95% confidence limits, calculated from data for representative isotopic compositions compiled by Rosman and Taylor[26] unless otherwise noted. [b] Error terms are one SE. [c] Range of isotope ratios as determined in eight samples by TIMS. Mass discrimination correction factor was determined in association with each sample measurement by ICPMS using NBS SRM-951 boric acid. [d] Data for all three magnesium isotopes were collected in each cycle (see Table 1). [e] Range of isotope ratios reported in four samples.[24] Mass discrimination correction factor was determined using NBS U-030 and U-050 uranium isotopic standards. Data for five uranium isotopes plus three additional masses were collected in each cycle (see Table 1).

an optimum dwell time ratio of ~4.72 for $^{115}In/^{113}In$ measurement ($R = 22.321 \pm 0.013$; see Table 3), as indicated by the minimum on the dotted curve in Figure 2. The experimental precision values deviate significantly from predictions based on the Poisson model. By accounting for the flicker noise contributions using eq 10, better agreement with the experimental data can be obtained, and an optimum dwell time ratio of ~2 is predicted for this particular case. However, Figure 2 suggests that the improvement in precision would be marginal.

Effect of Concentration on Precision. As manipulating the dwell time was found to be of little benefit for indium, $^{115}In/^{113}In$ representing the largest ratio investigated in initial stages of this work, experiments were then performed using $t_m/t_M = 1$ for four isotope pairs to study the effects of count rate on precision. In the context of tracer isotope studies,[8,9] or for determining the isotopic composition of materials of different origin,[7] it is of interest to note that no great advantage may actually result from varying t_m/t_M, within a defined total measurement time, as long as flicker noise makes a substantial contribution to the measurement uncertainty. Further analysis of sources of variation and measurement conditions are necessary, however, to fully evaluate this implication, particularly for isotope ratios substantially greater than that for indium.

The effects of increasing I_M, as a surrogate for concentration, on the RSE (%) values for four isotope pairs, without dead time and mass discrimination correction, are illustrated in Figure 3. Once again it can be seen that inclusion of the flicker noise contribution provides a more faithful description of the isotope ratio uncertainty than the Poisson model. For all isotope ratios, the uncertainties become fairly constant above I_M values of ~0.3 MHz, which contrasts with the expected behavior for counting statistics limited precision.[3]

Correction Factor Uncertainty Contributions. The results shown in Figure 3 do not provide a complete picture of all

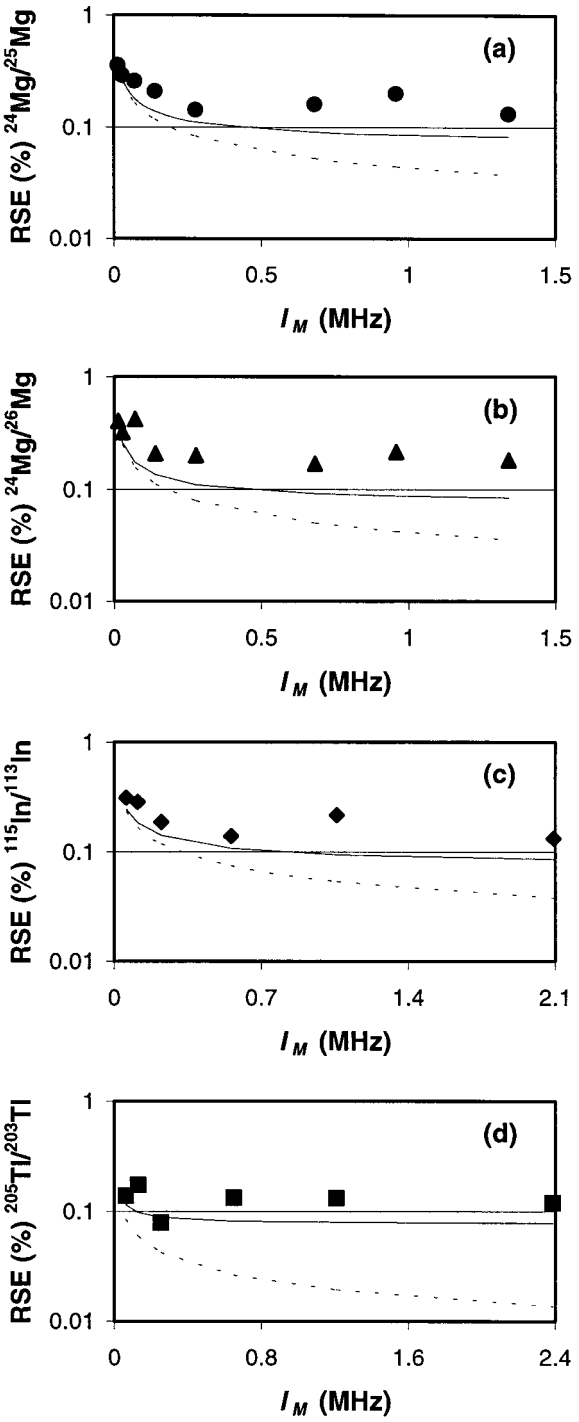

Figure 3. Effect of major isotope count rate on ratio precision for (a) $^{24}Mg/^{25}Mg$, (b) $^{24}Mg/^{26}Mg$, (c) $^{115}In/^{113}In$, and (d) $^{205}Tl/^{203}Tl$. Dotted lines show predictions made using the Poisson model of eq 9. Solid lines show the results of including the flicker noise contributions in eq 10. Experimental data are represented by solid symbols. Data have not been corrected for dead time and mass discrimination.

uncertainty contributions in isotope ratio measurements. So far, no consideration has been given to the effects of dead time and mass discrimination correction. Correction of raw isotope ratio data is, of course, mandatory to prevent systematic errors in the results.[4,11,20] It is necessary to determine the magnitude of the dead time and mass discrimination experimentally, and, as such, the correction factors have associated uncertainties. In Table 3,

results from the experimental determination[14] of these factors are summarized. It should be mentioned at this point that τ and κ were computed using the same data sets as utilized in plotting Figure 3. The data of Table 3 illustrate that each dead time value carries a substantial error term, the RSE varying between 3.5 and 17.6%.

Hayes and Schoeller[10] recognized the importance of uncertainties in the dead time for high-precision pulse counting over 20 years ago. An important finding was that, for ratio measurements, precision is limited by the difference between the count rates obtained for the two isotopes. This is manifest in the final term on the right-hand side of eq 13. As this difference approaches a minimum, i.e., for equal isotopic abundance, then the uncertainty contribution of the dead time will tend to zero.[10,11] If the additional effects of mass discrimination uncertainty, given by the third term on the right-hand side of eq 13, are contemplated, it becomes obvious that this term is also minimized at $R = 1$.

The RSE values of the mass discrimination correction factors in Table 3, ranging from 0.02 to 0.35%, demonstrate the significantly better precision with which this variable can be determined. The calculated uncertainties include contributions from uncertainties in measured data for the natural abundances of the isotopes,[26] as standard solutions assumed to have natural isotopic compositions were used for these measurements (except boron and uranium; see below). It would be possible to reduce such uncertainty contributions by using high-quality reference materials having more precisely measured isotopic compositions.

Plots of RSE values for τ and κ corrected isotope ratios, again as a function of I_M, are shown in Figure 4. Applying eq 15 to the experimental RSE values, to account for uncertainties in the correction factors, shifts the data points further away from the curve showing the behavior expected of counting statistics limited measurement. Comparing the corrected and uncorrected experimental data, it can be seen that there is a discernible I_M value at which the uncertainty in the determined ratio is at a minimum, for each of the isotope pairs. This trend is also reflected in the model accounting for τ and κ uncertainty contributions, as well as flicker noise, eq 14. Figure 4 also shows that this model is capable of providing fairly accurate predictions of the experimental uncertainties.

The importance of τ and κ for providing a complete assessment of uncertainties in ICPMS ratio measurements is implied by the differences between the uncorrected and corrected experimental RSE values in Figure 4. A breakdown of the relative contributions made by the components of eq 14 to the total uncertainty for two of the isotope ratios is provided in Figure 5. The patterns observed for $^{24}Mg/^{26}Mg$ and $^{115}In/^{113}In$ were similar to those for $^{24}Mg/^{25}Mg$ shown in Figure 5a and have therefore been omitted. It can be seen that although dead time is the variable that is least precisely determined (refer to Table 3), it is only at major isotope count rates in excess of 1 MHz that its effect on the RSE of the ratio becomes dominant. Instead, it is the uncertainty associated with κ that largely determines the overall precision.

Results for the two magnesium ratios in Figure 4 show that the precision values for $^{24}Mg/^{25}Mg$ are better than those for $^{24}Mg/^{26}Mg$, despite the fact that R is somewhat lower for the latter isotope pair. This can be rationalized in terms of the greater elapse time required to complete each measurement for $^{24}Mg/^{26}Mg$ when data for ^{25}Mg are also sampled.[3,15,18] As such, f_c is located in a lower frequency region accepting more flicker noise (see Figure 1), which is detrimental to the precision of the correction factor evaluation, as seen in Table 3, as well as to the uncertainties in the Q values. The minimum points on the R_{corr} curves in Figure

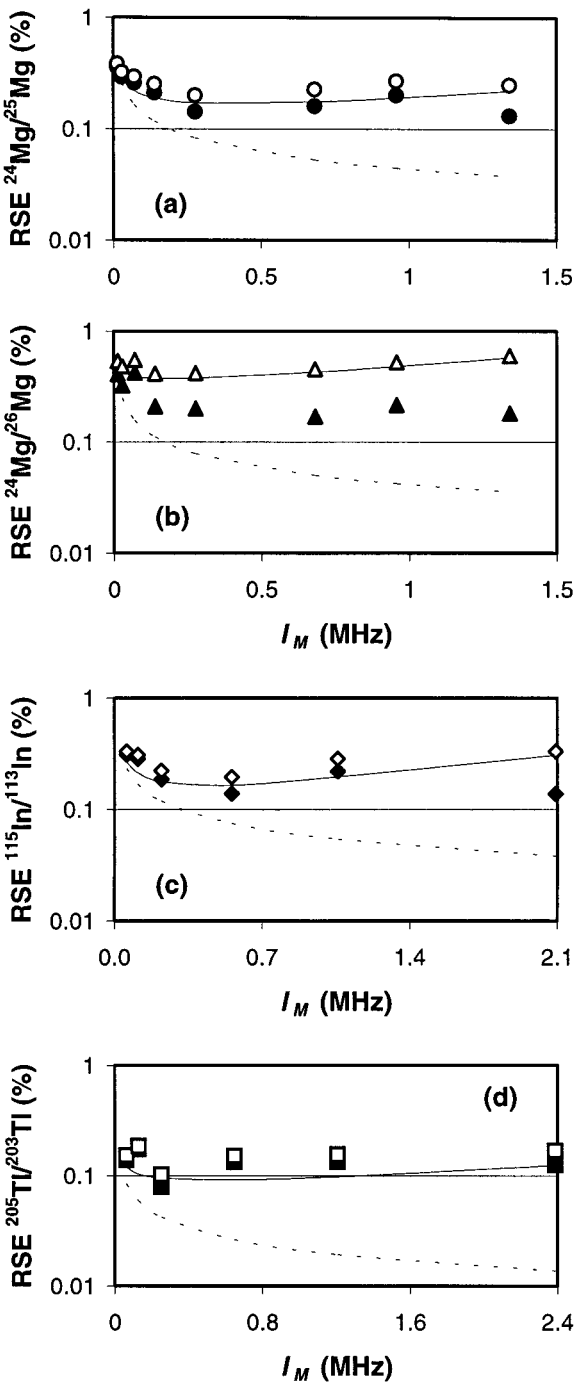

Figure 4. Effect accounting for uncertainties in dead time and mass discrimination correction factors on ratio precision as a function of major isotope count rate for (a) $^{24}Mg/^{25}Mg$, (b) $^{24}Mg/^{26}Mg$, (c) $^{115}In/^{113}In$, and (d) $^{205}Tl/^{203}Tl$. Dotted lines show predictions made using the Poisson model of eq 9. Solid lines have been computed using eq 14. The filled symbols are the raw experimental RSE values for the ratios, R_{expt}; the open symbols include the uncertainty contributions from dead time and mass discrimination correction, according to eq 15.

(26) Rosman, K. J. R.; Taylor, P. D. P. *Pure Appl. Chem.* **1998**, *70*, 217−236.

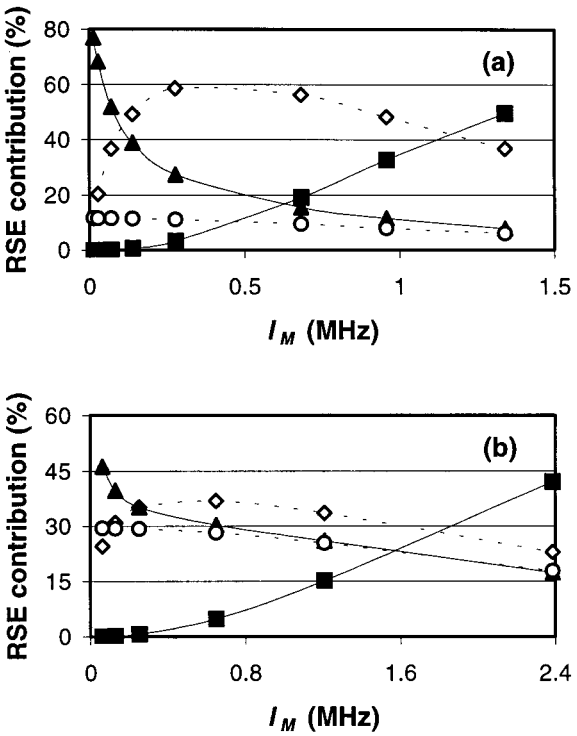

Figure 5. Relative contributions (%) made by the components of eq 14 to the RSE in the (a) $^{24}Mg/^{25}Mg$ and (b) $^{205}Tl/^{203}Tl$ isotope ratios as a function of major isotope count rate. Filled triangles denote contributions made by $u(Q_m)^2$, open circles $u(Q_M)^2$, open diamonds $u(\kappa)^2$ and filled squares $u(\tau)^2$.

4 all approach the corresponding RSE values for the mass discrimination correction factors of Table 3. This emphasizes the importance of evaluating κ as precisely as possible, suggesting that high-quality isotopic reference materials should be more frequently applied in ratio measurements by ICPMS than is currently the case.

Of interest is the fact that at the highest count rate, for the $^{205}Tl/^{203}Tl$ results in Figure 5b, the uncertainty contribution from measurement of the major isotope is actually slightly greater than that for the minor isotope. This is a consequence of a substantial flicker noise contribution to measurements made at such high count rates.

Importance of Including Correction Factor Uncertainties. As an example of the impact of correction factor uncertainties in method comparison studies, results for boron isotope ratios determined by ICPMS and TIMS[23] are plotted in Figure 6a. Application of the *t*-test[25] initially revealed highly significant differences ($P > 0.005$) between the results for seven out of eight samples. By considering the uncertainty contributions made by τ and κ correction of the raw data generated by ICPMS, it was ascertained that the isotope ratio for only one sample still deviated significantly from that obtained by TIMS.

For all but two of the samples, boron concentrations were sufficiently high to yield major isotope count rates in the range of 0.5−2.5 MHz. As such, it might be expected that the precision would only be limited by counting statistics. However, analysis of the uncertainty contributions showed that counting statistics accounted for ~40 and ~10% of the total variance at count rates of 0.05 and 0.2 MHz, respectively. At the higher major isotope count rates recorded for the remaining samples, more than 98.5% of the variance was attributable to correction factor uncertainties.

It was noted that mass discrimination varied strongly on a day-to-day basis for boron isotope ratio measurement (see Table 3). Such variation will obviously impair both the accuracy and precision of isotope ratio measurements of lighter elements by ICPMS and highlights the need to carefully assess the magnitude of uncertainties contributed by the correction factors.

For the results of uranium isotope ratio measurement by ICPMS, shown in Figure 6b, better accuracy and precision was obtained than for boron. In the high-mass region, greater instrument stability results in reduced error contributions from the mass discrimination correction factor. On average, RSE ($R_{expt,corr}$) values calculated using eq 15 for the four NUSIMEP-2 samples[24] were ±0.15 and ±0.10% for the $^{234}U/^{238}U$ and $^{235}U/^{238}U$ ratios, respectively. The major contributor to the uncertainties in the $^{235}U/^{238}U$ ratios determined by ICPMS was the mass discrimination correction factor (>93%). For the $^{234}U/^{238}U$ ratios, the number of minor isotope counts accumulated accounted for between 5 and 27% of the variance, but the uncertainty associated with mass discrimination correction remained the limiting factor for measurement precision.

CONCLUSIONS

Deviations of experimental isotope ratio precision, from that expected on the basis of counting statistics, can be quantitatively interpreted in terms of flicker noise contributions using the model presented in eq 10. Using an ICPMS instrument equipped with a quadrupole mass filter, Begley and Sharp[3] noted that accumulating a greater number of counts, by increasing either the number of scans or the analyte concentration, did not improve the precision as dramatically as hoped. It was suggested that this was probably a result of instrumental drift, which is certainly likely to present a greater potential source of uncertainty when a quadrupole-based system is utilized. Begley and Sharp[3] did, however, also indicate that variations in the degree of mass discrimination could contribute to isotope ratio uncertainties. Although the effects of drift are not accounted for in the model described, the present analysis suggests that flicker noise could equally well explain the observed behavior, as shown in Figure 3. By operating the double-focusing type of instrument employed in this work in low-resolution mode, drift problems are generally minimal over the measurement time scales employed here, as flat-topped peaks are generated.[19] A recent account of the use of a time-of-flight ICPMS instrument for isotope ratio measurements has also demonstrated deviations from the Poisson model on increasing the number of counts acquired.[27] Thus, the present analysis of sources of uncertainty is probably generally applicable to a range of instruments used for isotopic measurements by mass spectrometry.

It is generally accepted that major isotope count rates should not be too high, to prevent the introduction of large uncertainties by dead time correction of the raw data.[28,29] Clearly, the effects of flicker noise are also important in this context. Consideration of

(27) Vanhaecke, F.; Moens, L.; Dams, R.; Allen, L.; Georgitis, S. *Anal. Chem.* **1999**, *71*, 3297−3303.
(28) Monna, F.; Loizeau, J.-L.; Thomas, B. A.; Guéguen, C.; Favarger, P.-Y. *Spectrochim. Acta* **1998**, *53B*, 1317−1333.
(29) Vanhaecke, F.; de Wannemacker, G.; Moens, L.; Dams, R.; Latzoczy, C.; Prohaska, T.; Stingeder, G. *J. Anal. At. Spectrom.* **1998**, *13*, 567−571.

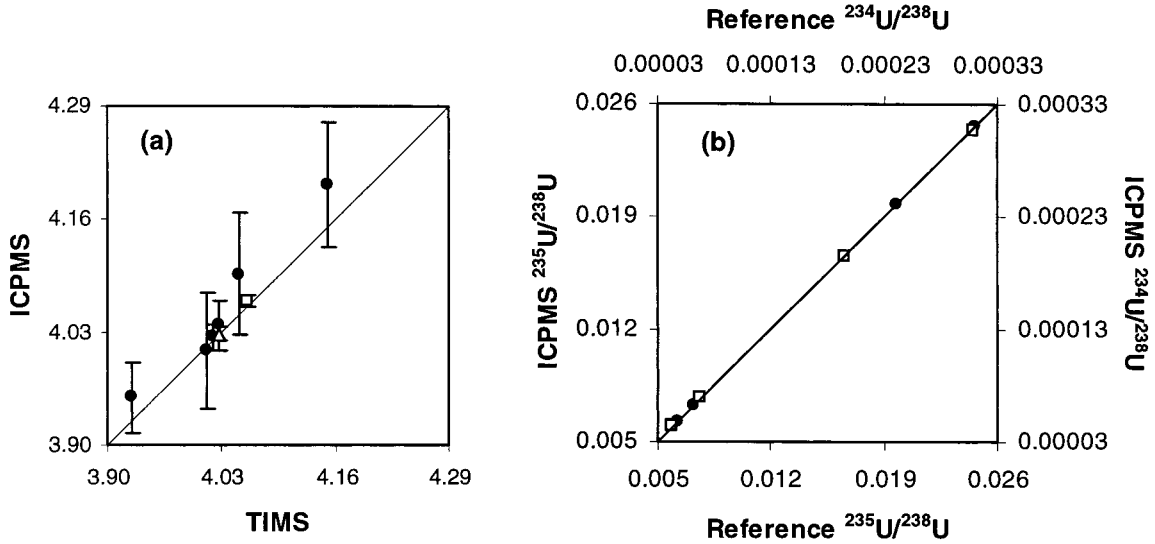

Figure 6. Comparison of (a) $^{11}B/^{10}B$ and (b) $^{234}U/^{238}U$, $^{235}U/^{238}U$ ratios for ICPMS with TIMS data and reference values, respectively. (a) No significant difference (*t*-test; 99% confidence level[25]) between the determined isotope ratios was observed for the sample marked with an open triangle when only the ICPMS measurement uncertainties are considered. Samples denoted by filled circles provided significantly different results unless uncertainty contributions from τ and κ were included in the analysis (see Table 3). Results for the final sample, shown by an open square, are significantly different ($P > 0.03$) even after inclusion of correction factor uncertainties. Error bars are 95% confidence intervals for the ICPMS ratios; TIMS uncertainties are smaller than the data points. (b) Data for $^{234}U/^{238}U$ ratios are denoted by open squares and for $^{235}U/^{238}U$ by filled circles for four NUSIMEP-2 samples.[24] No significant differences were detected; uncertainties are smaller than the data points. Solid lines in (a) and (b) represent perfect agreement between the methods.

flicker noise and dead time correction suggests that count rates should not exceed ~0.3 MHz, if high-precision isotope ratios are to be determined by ICPMS (see Figures 4 and 5). Comparison of sources of uncertainty indicates that, for precise isotope ratio measurement by ICPMS, the most crucial single factor is the mass discrimination correction factor. Notably, this factor is also of fundamental importance in determining the accuracy of the measured isotope ratio.[11] Finally, it should be mentioned that the approach described, for quantifying contributions to isotope ratio uncertainties, will be of value in developing rational optimization strategies for high-precision measurement using single-collector ICPMS.

ACKNOWLEDGMENT

Initial stages of this work were financially supported by TFR (Technical Research Council), Sweden. SGAB Analytica, Luleå, Sweden, provided economic and technical assistance. Thanks are due to Irina Rodushkina (SGAB Analytica) for careful revision of the mathematical expressions.

Received for review December 29, 2000. Accepted April 8, 2001.

AC001537Y